

# **Seismological Characterization of the 2021 Yangbi Foreshock-Mainshock Sequence, Yunnan, China: More than a Triggered Cascade**

**Yijian Zhou<sup>1\*</sup>, Chunmei Ren<sup>2</sup>, Abhijit Ghosh<sup>1</sup>, Haoran Meng<sup>3</sup>, Lihua Fang<sup>4\*</sup>, Han  
Yue<sup>2</sup>, Shiyong Zhou<sup>2</sup>, and Youjin Su<sup>5</sup>**

<sup>1</sup>Department of Earth and Planetary Sciences, University of California, Riverside, California, USA

<sup>2</sup>Institute of Theoretical and Applied Geophysics, Peking University, Beijing, China.

<sup>3</sup>Southern University of Science and Technology, Guangdong, China

<sup>4</sup>Institute of Geophysics, China Earthquake Administration, Beijing, China

<sup>5</sup>Yunnan Earthquake Agency, Yunnan, China

## **Contents of this file**

Text S1

Figures S1 to S17

Table S1 to S2

## **Introduction**

This supporting information provides additional details on the multi-point-source inversion process, source spectrum analysis, and Coulomb stress modelling.

## **Text S1**

Tests on MPS inversion process for the largest foreshock. We demonstrate the necessity of using two subevents for the largest foreshock by presenting the inversion result with different search windows. First, we tried single subevent to fit the observations. We set the time window to 0-10s, and results show that synthetic waveforms can fit only the initial seismic phase and first 1-2 wiggles, yet the remaining unfitted waveforms resembles another seismic event (Figure S14). Instead, when the time window is given posterior, from the initiation 3-10s, the synthetics are coherent with major peaks, while the initial phase becomes reversed (figure S13), resulting in an absolutely opposite mechanism (i.e. left-lateral). Therefore, we add another subevent to simulate the rupture process of the foreshock on the basis of the solution exhibit in figure S10a.

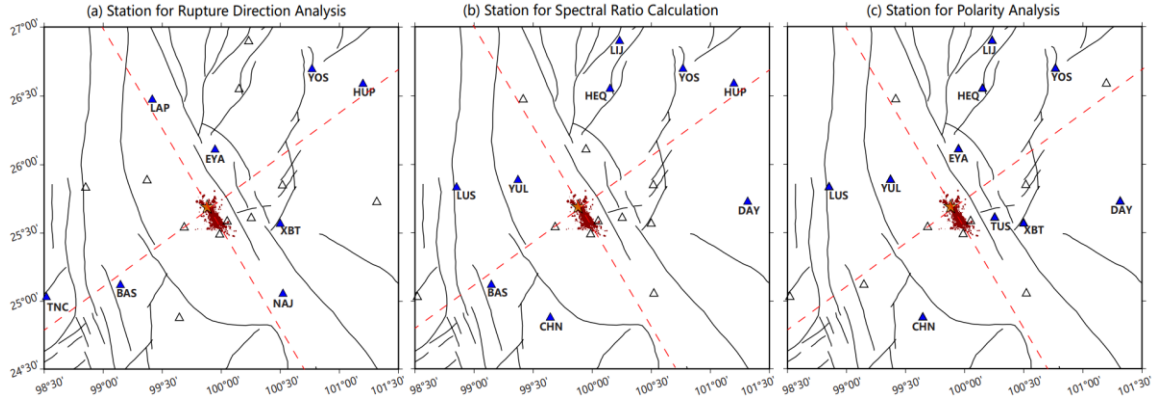


**Figure S1.** Stations used for different analysis. (a), (b), and (c) plot stations for rupture direction analysis, spectral ratio calculation, and for polarity analysis, respectively. The blue triangles with the names annotated is the selected stations, and the hollow black triangles are stations not selected. The red dashed lines mark the nodal plane direction of the mainshock.

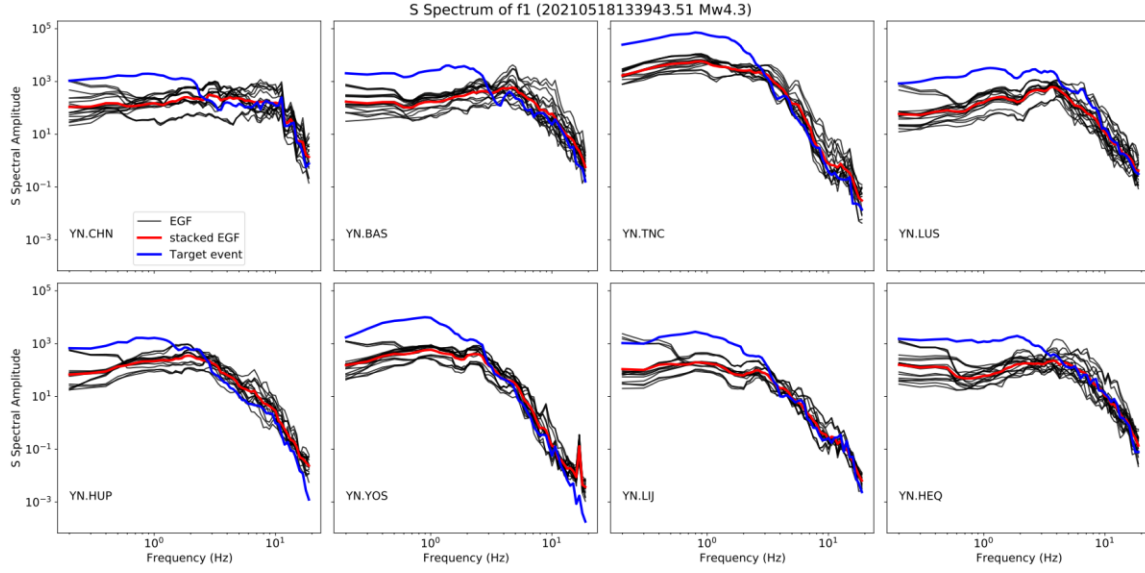


**Figure S2.** Spectral amplitudes of *f1*. The spectral amplitude of EGF, stacked EGF, and target events are plotted in black, red, and blue lines, respectively. Each subplot shows results on one station.

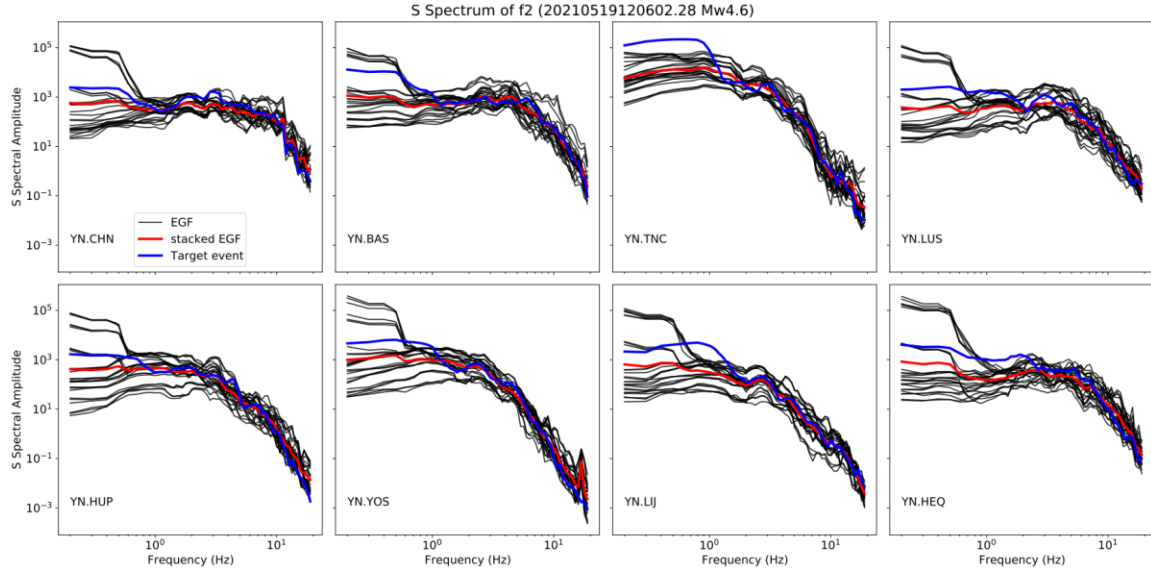


**Figure S3.** Spectral amplitudes of  $f_2$ . The markers have the same meaning as that in Figure S2.

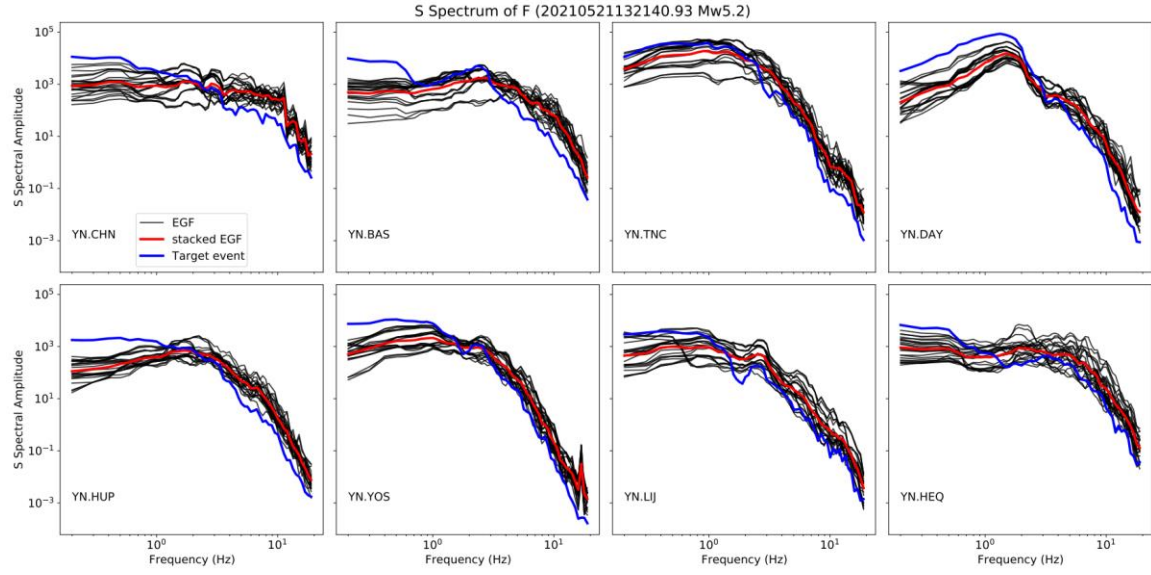


**Figure S4.** Spectral amplitudes of *F1*. The markers have the same meaning as that in Figure S2.

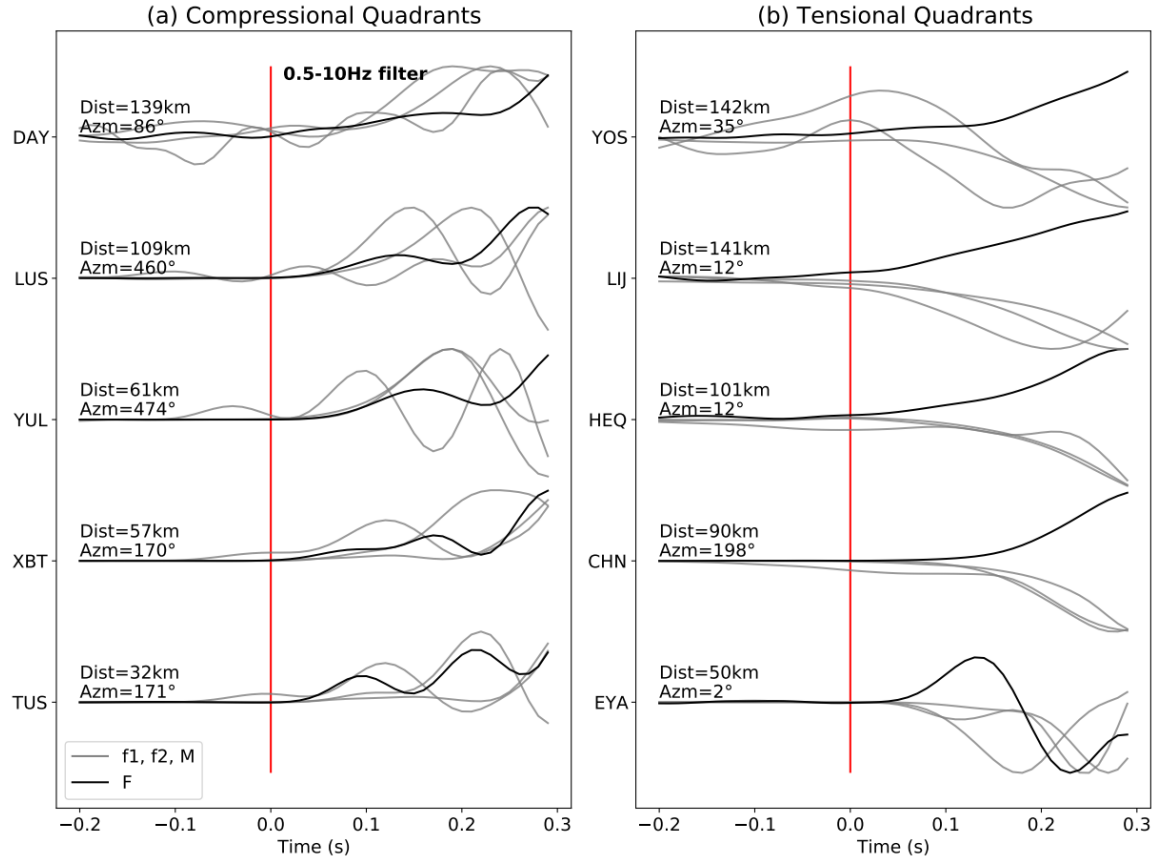


**Figure S5.** Polarization of *FI* records. (a) & (b) plot stations in the compressional and tensional quadrants, respectively. The gray lines plot P wave of major events on *Fault\_M*, i.e. *f1*, *f2*, and *M*; black lines plot that of *FI*. The P-wave is obtained by first bandpass filter a 30-s window by 0.5-10Hz, and slice to a zoom-in window.

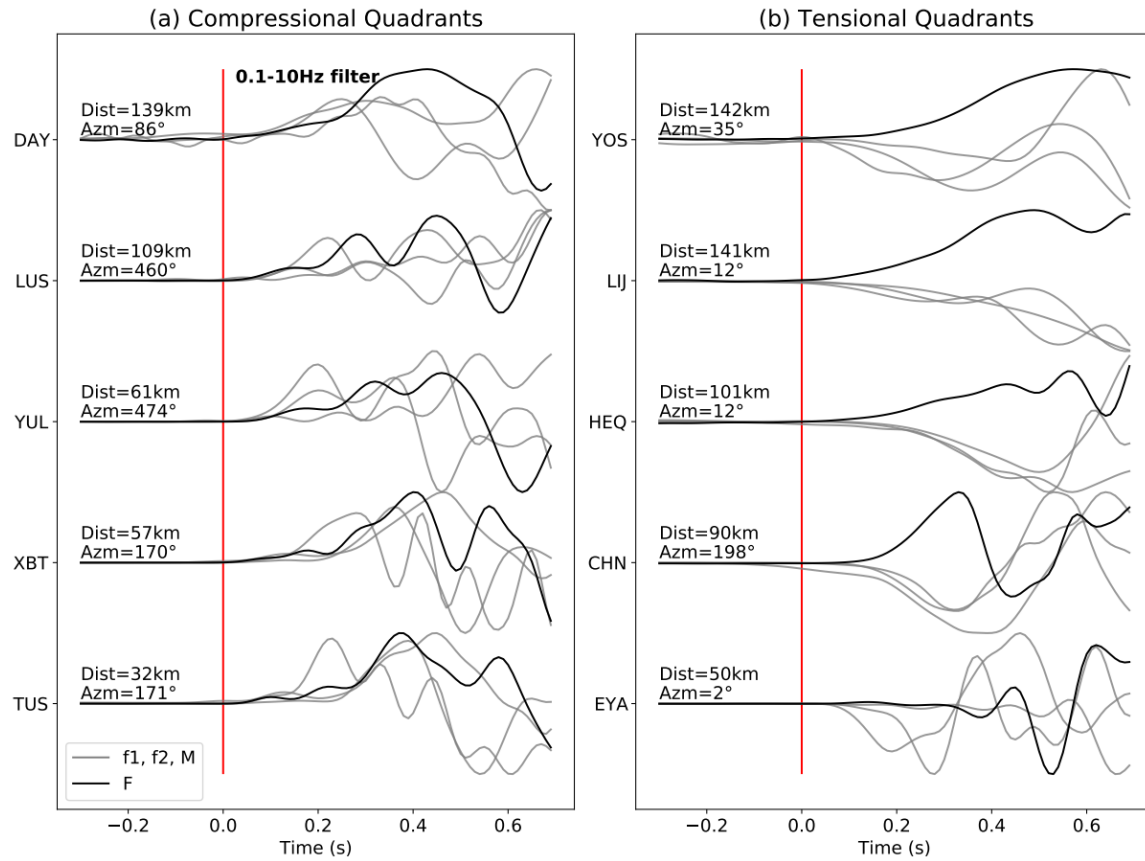


**Figure S6.** Same as Figure S5, but with longer window and lower frequency band.



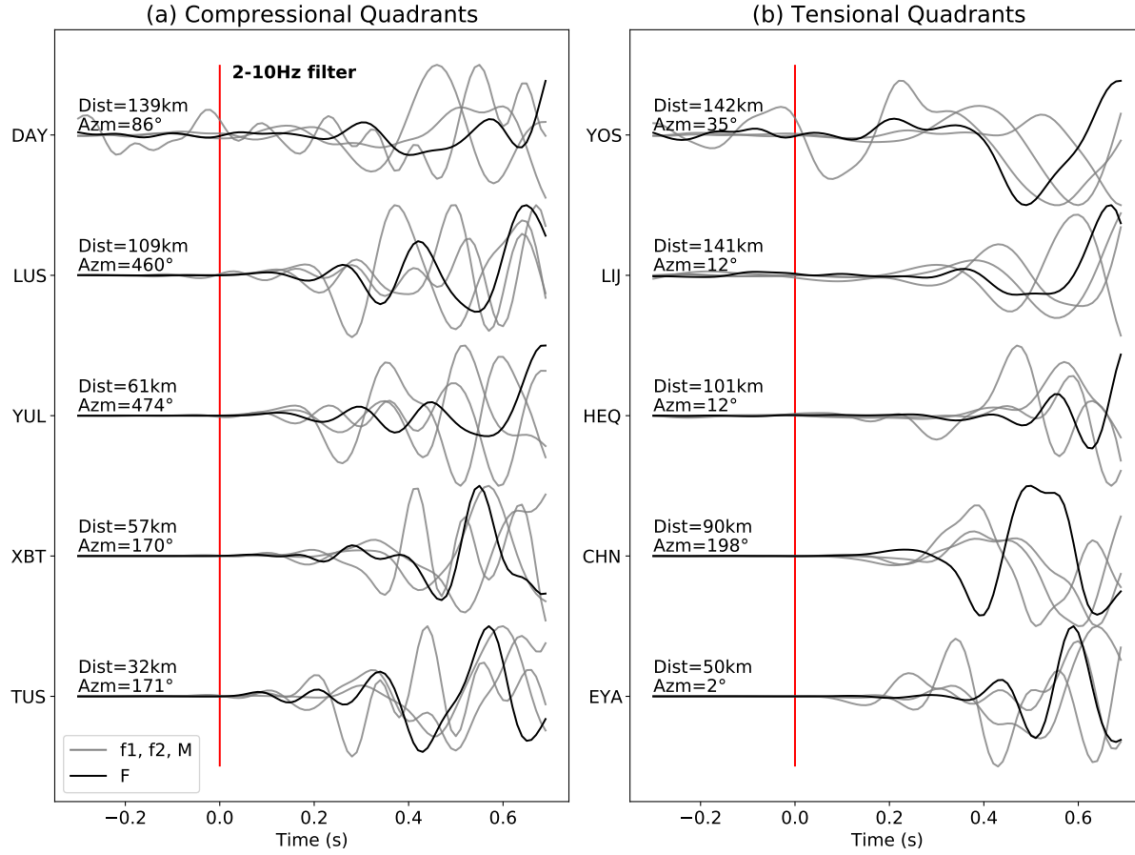


**Figure S7.** Same as Figure S5, but with longer window and higher frequency band.

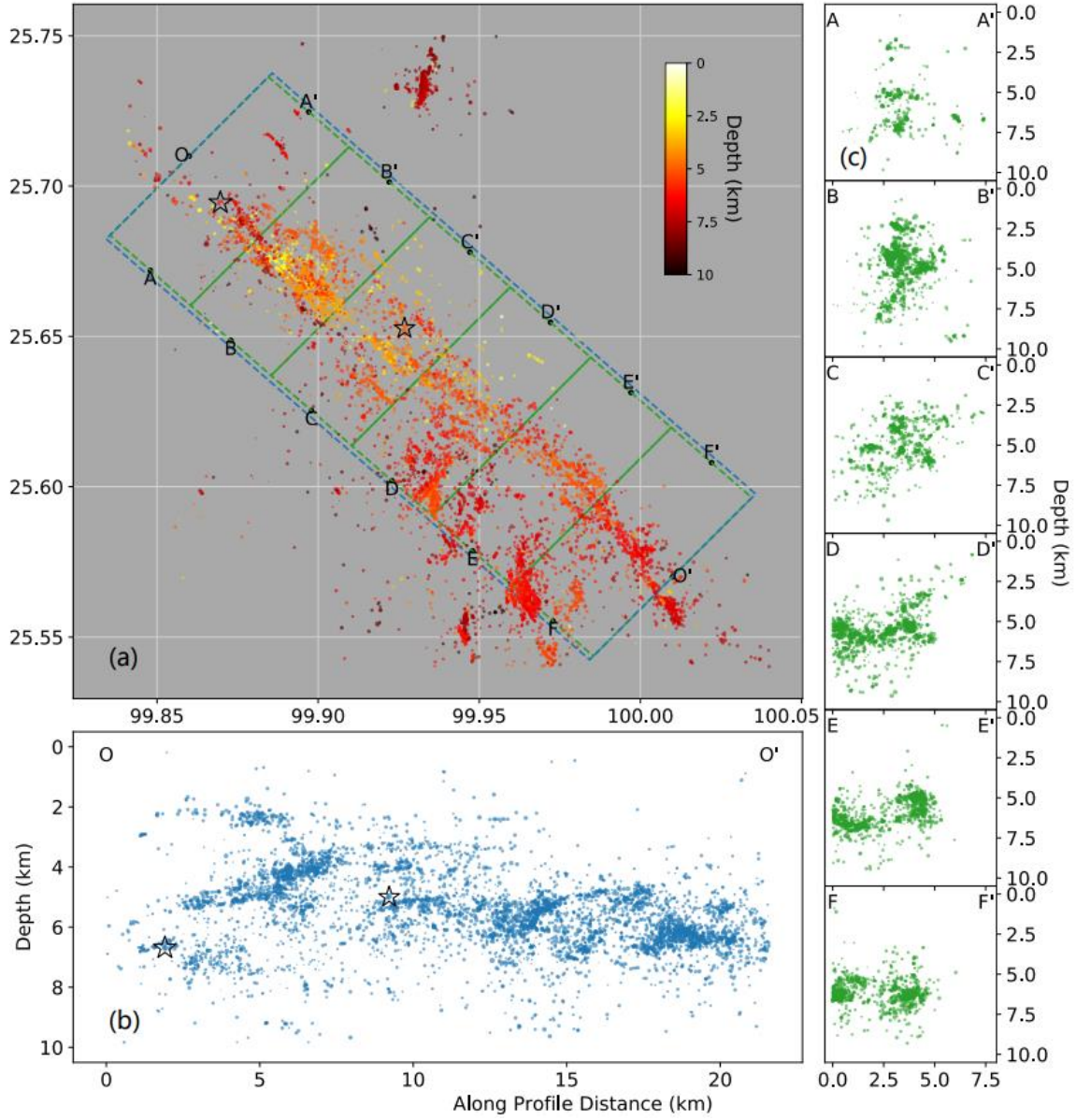


**Figure S8.** Distribution of Yangbi aftershocks from 17<sup>th</sup> May to 28<sup>th</sup> May. (a), (b), and (c) show map view, along-strike cross-section, and fault-vertical cross-sections, respectively. seismic events are plot in dots with the size scaled by its magnitude. The hypocentral depth in (a) is represented by color. Location of the mainshock *M* and the largest foreshock *F* is plotted in hollow stars.

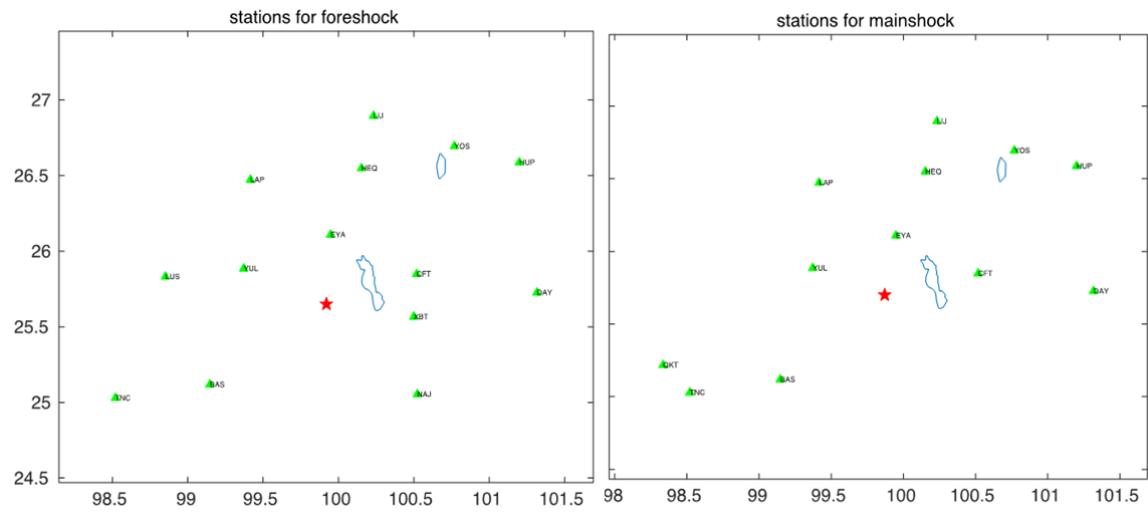


**Figure S9.** Stations for MPS inversion.

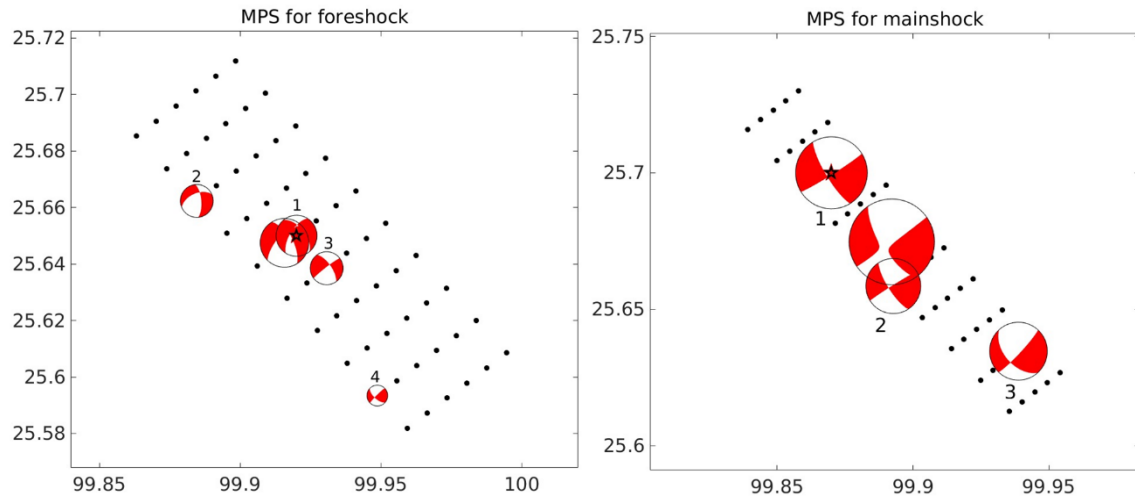


**Figure S10.** MPS inversion result. The black dots are the preset mesh grids. The black star marks the epicenter.

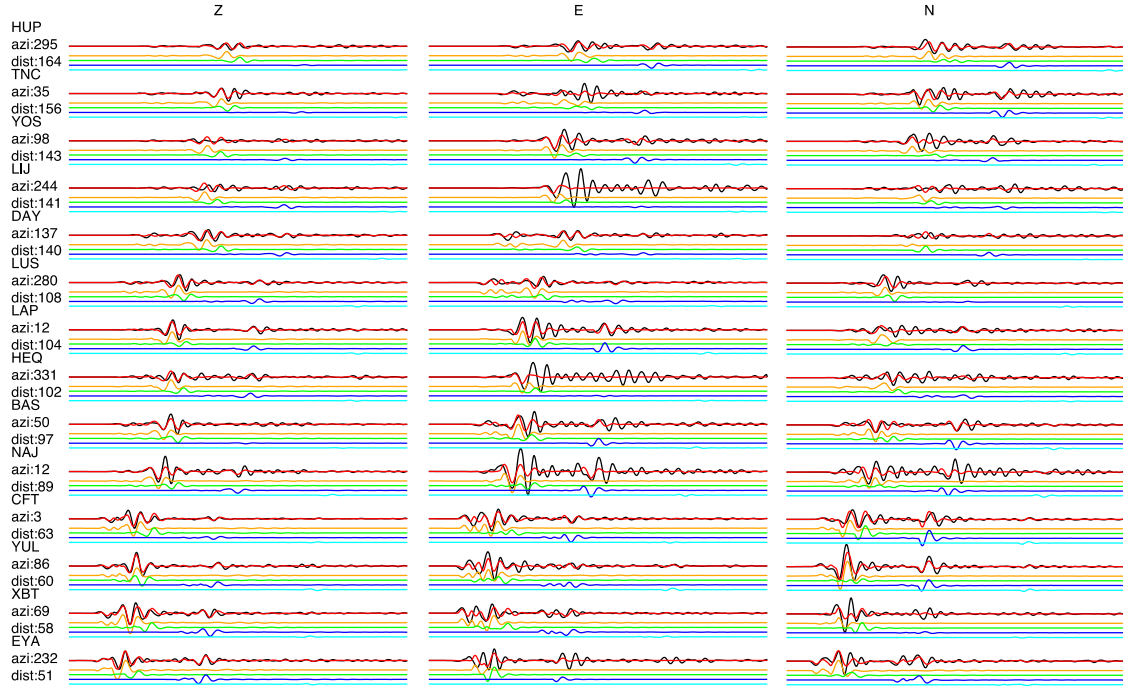


**Figure S11.** MPS waveform fitting for the largest foreshock. The black and red lines are the observation and predicted waveforms. The waveforms below in other colors are that predicted by each subevents.

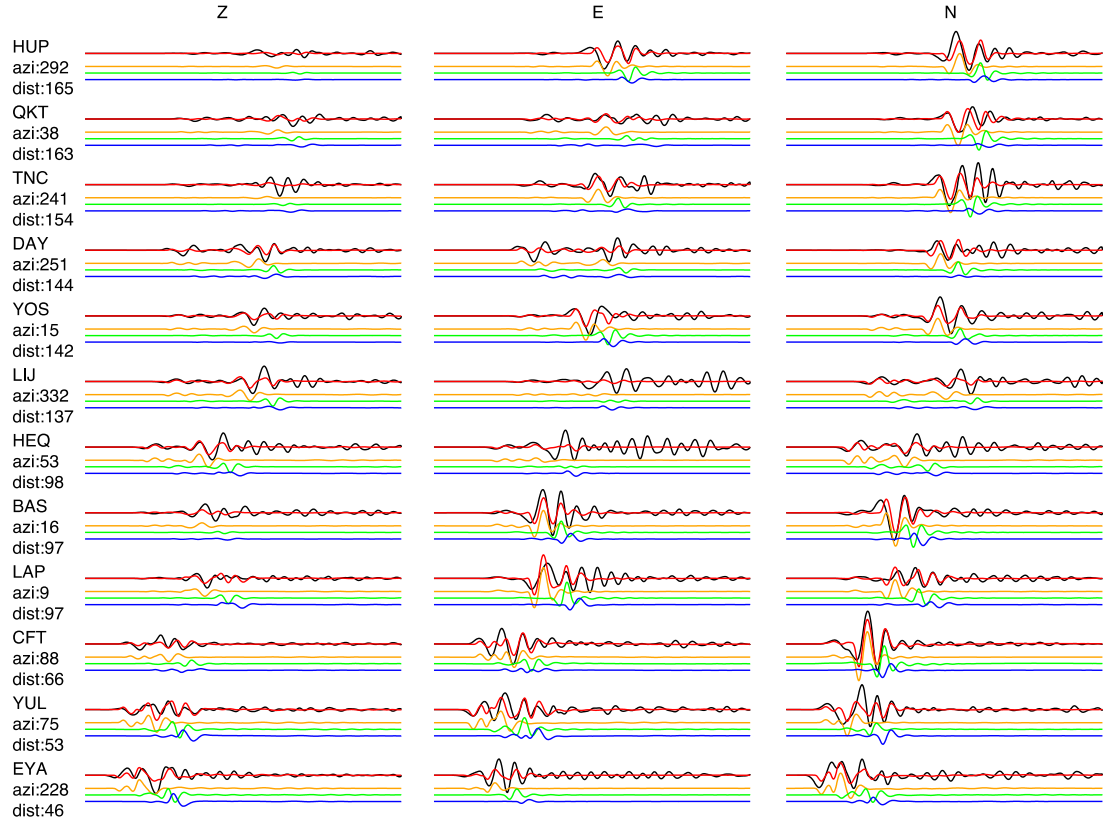


**Figure S12.** MPS waveform fitting for the mainshock. The symbols have the same meaning with Figure S11.

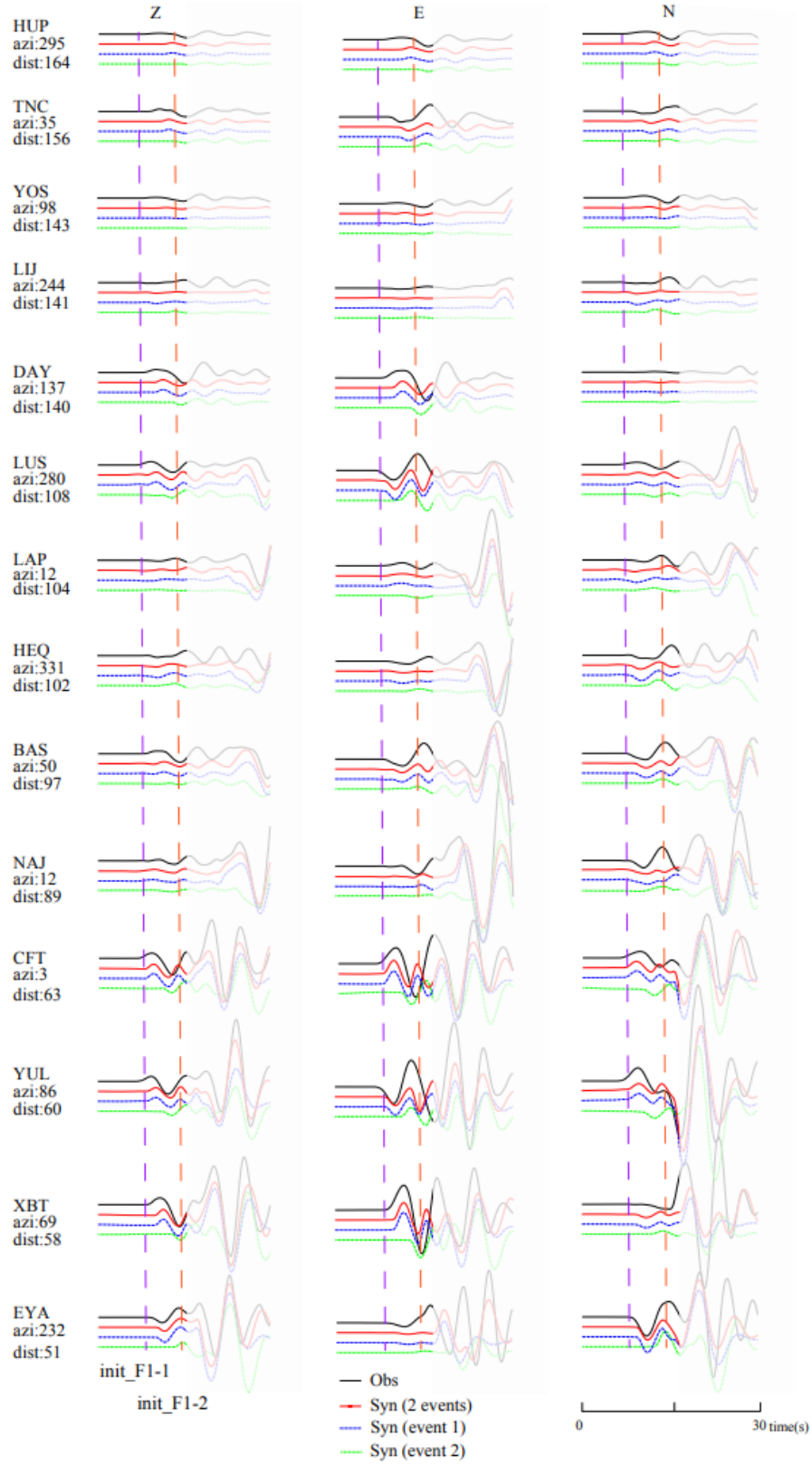


**Figure S13.** Comparison of MPS inversion result for  $F1$  with different choices of searching window. The purple and red vertical dashed lines plot the P arrival of  $F1_1$  and  $F1_2$ .

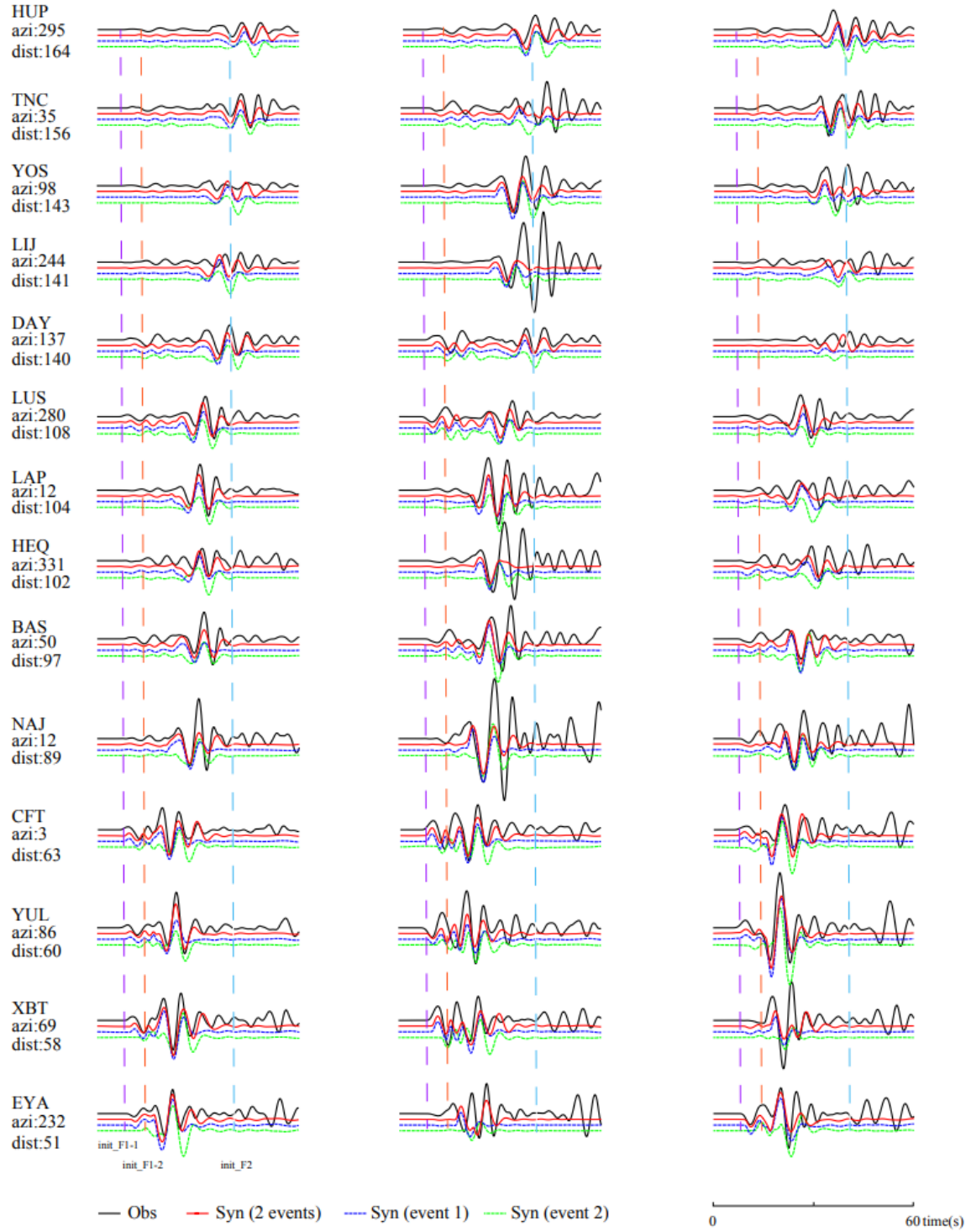


**Figure S14.** Same as Figure S13, but show longer window.



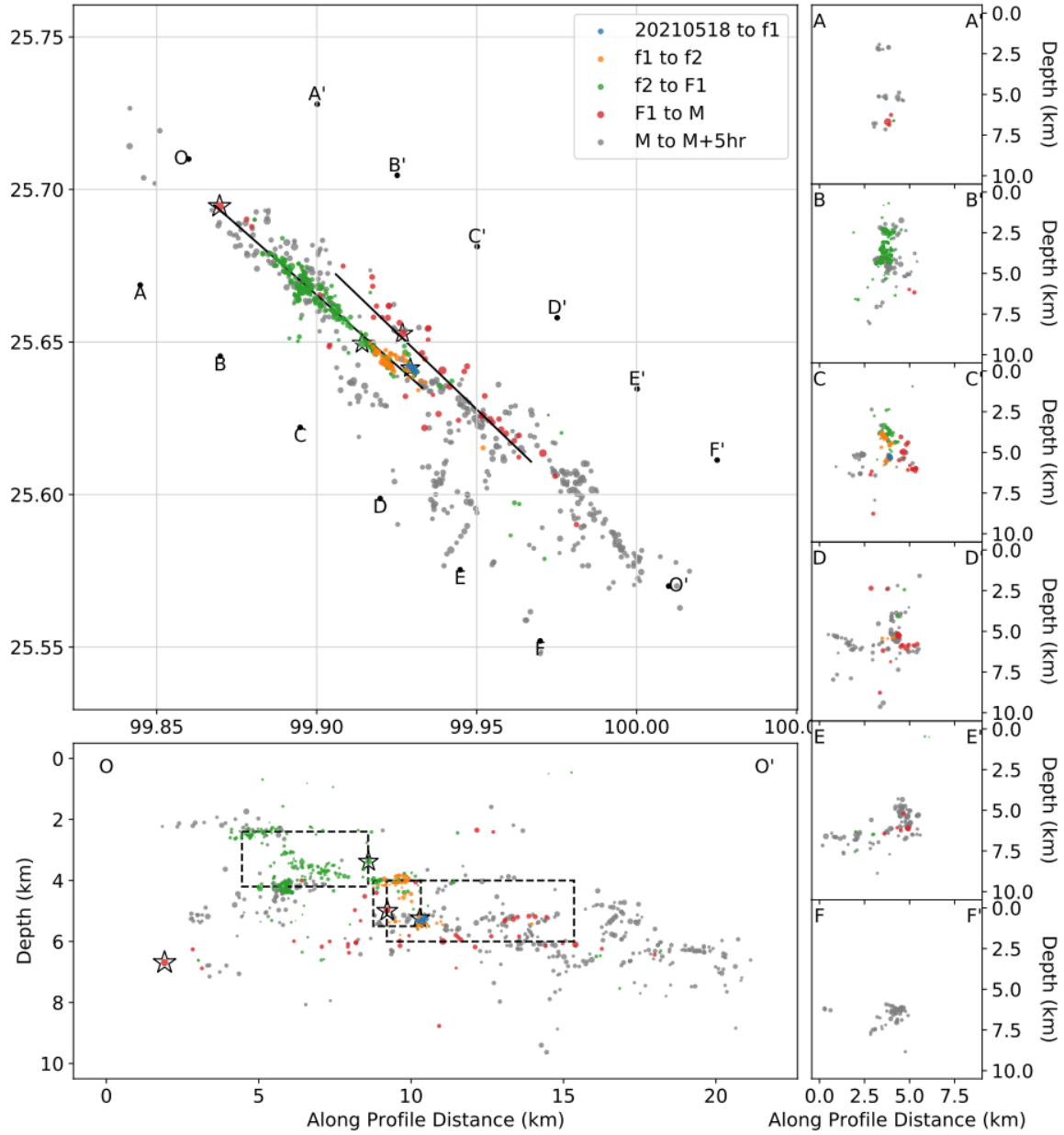


**Figure S15.** Fault model for a pure-unilateral  $FI$  rupture. The symbols have the same meaning as in Figure 7.

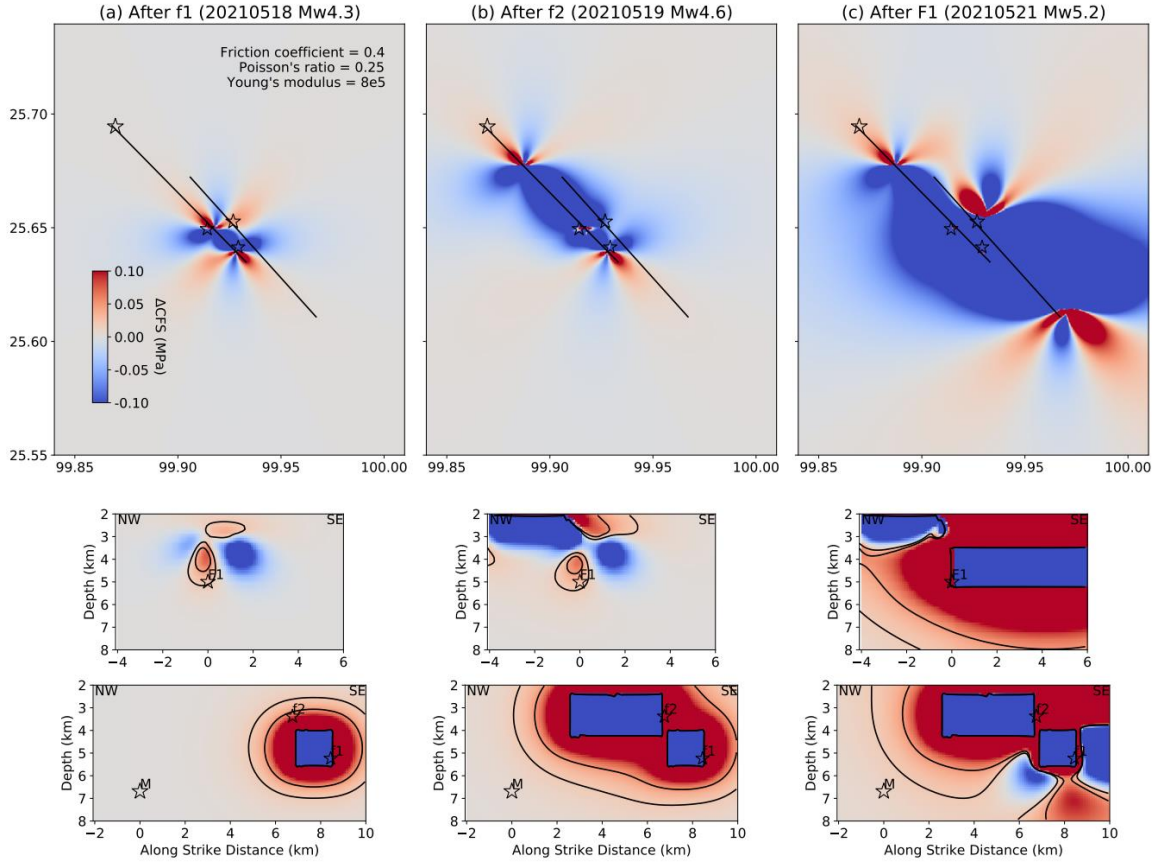


**Figure S16.** Coulomb stress evolution with *F1* as a purely uni-lateral rupture. The symbols have the same meaning as in Figure 8.

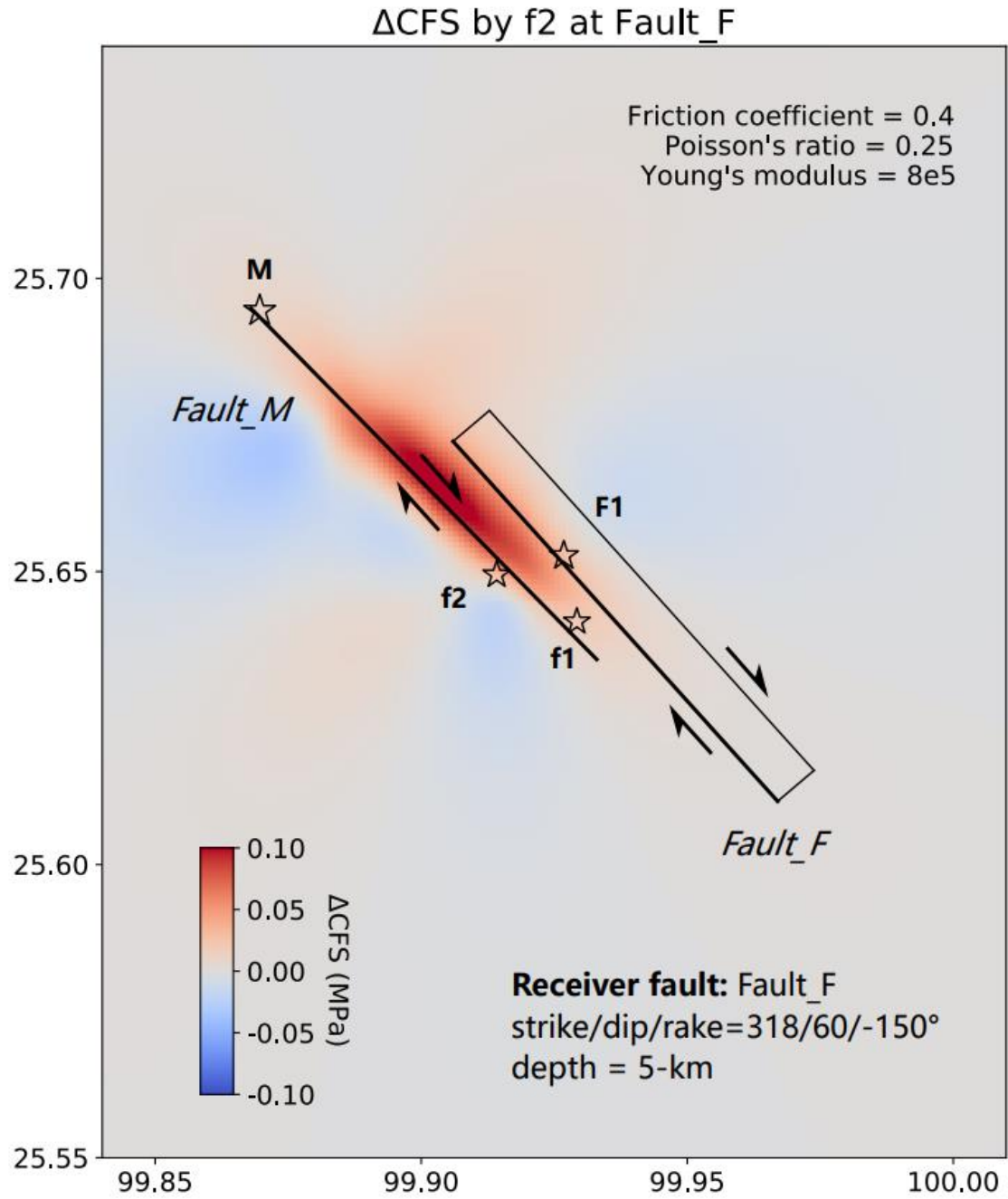


**Figure S17.** Coulomb stress change induced by  $f_2$  with *Fault\_F* as the receiver fault at a depth of 5-km.

**Table S1.** MPS result of the largest foreshock

<b>Subevent</b>	<b>Time(s)</b>	<b>Location(lat/lon/dep)</b>	<b>Mechanism(strike/dip/rake)</b>		<b>M<sub>w</sub></b>
1	0.0	25.65/99.92/15.0	320/56/-148	211/63/-37	5.1
2	5.2	25.66/99.88/13.5	354/67/-138	246/52/-29	4.8
Sum 1&2	2.2	25.65/99.91/14.5	332/58/-142	220/58/-38	5.1
3	31.2	25.64/99.93/15	324/67/-174	232/84/-22	4.9
4	69.2	25.59/99.95/13.5	224/84/26	132/63/174	4.4
Sum all	12.1	25.65/99.92/14.6	328/62/-151	224/64/-30	5.2

**Table S2.** MPS result of the mainshock

<b>Subevent</b>	<b>Time(s)</b>	<b>Location(lat/lon/dep)</b>	<b>Mechanism(strike/dip/rake)</b>		<b>M<sub>w</sub></b>
1	0.0	25.70/99.87/17.0	148/77/-175	57/85/-12	5.7
2	5.9	25.66/99.89/7.1	237/87/15	147/74/177	5.4
3	8.4	25.63/99.94/8.4	138/51/-171	43/83/-39	5.5
Sum	4.4	25.67/99.89/16.1	145/70/-177	55/87/-19	5.8